



Chapter 27

Structural Health Monitoring on Industrial Structures Using a Combined Numerical and Experimental Approach

Fabian Keilpflug, Robert Kamenzky, Daniel J. Alarcón, Tarun Teja Mallareddy, and Peter Blaschke

Abstract The Brandenburg industrial landscape is characterized by heavy industry sectors such as metallurgy and mining. Most of these industrial plants (ironworks, refineries, mines, etc.) have their origin in the state-planned rapid industrialization the German Democratic Republic underwent during the 1950s. Therefore, many critical constructive parts of these industrial plants have already surpassed their life expectancy or its remaining life expectancy can no longer be clearly determined due to poor documentation.

Heavy duty bridge cranes are an essential part of heavy industries or warehouses. During the course of their lives, these cranes and their rails are exposed to many different loads, damages and material fatigue processes during operation. Runway beams, those where the bridge crane runs on, are especially prone to the generation of cracks due to material fatigue. Condition monitoring and early damage detection can ensure the long-term load capacity and serviceability of bridge cranes, and contribute to a more cost-effective maintenance.

This paper presents the results of a feasibility study for a vibroacoustic damage detection procedure on bridge crane runway beams. A segment of a railway beam has been studied with experimental modal analysis and the results used to correlate and validate a FE model, generated by means of optical scanning. The modal analysis was performed by means of automatic impact excitation and Scanning Laser Doppler Vibrometry. Several damage cases were later simulated in the FE model, evaluating this way the development potential for a vibroacoustic method for damage detection in bridge crane railway beams.

Keywords Structural health monitoring · Overhead crane · Beam · Scanning Laser Doppler Vibrometry · Damage detection

27.1 Historical Introduction

Brandenburg, a federal state in Germany's northeast region, has traditionally been an agricultural powerhouse. The nineteenth century brought a rapid industrialization to the region, mainly due to its proximity with the German capital Berlin and its efficient waterways. The World War II and its aftermath deeply damaged the region's industrial panorama, which needed to be rebuilt almost from scratch. During the second part of the twentieth century, the German Democratic Republic was founded, being in practice a puppet state from the Soviet Union. The Soviet industrial policy gave an important focus on heavy industry sectors such as mining, metallurgy and oil refining. This heavy and rapid re-industrialization took place in a matter of 20–25 during the decades of 1950s and 1960s [1, 2]. This has severe implications nowadays:

1. These industrial complexes and their largest components and structures are about 50–70 years old and therefore, are very close to the end of their planned service lives.
2. Accurately determining the service life from these structures is a challenging task. Such a rapid industrialization driven by foreign officials implied very poor project documentation. In the worst cases this documentation was lost after the political changes that East Germany and the Soviet Union underwent during the 1980s and 1990s.

F. Keilpflug · R. Kamenzky · D. J. Alarcón (✉) · T. T. Mallareddy
Laboratory for Machine Dynamics and NVH, Technical University of Applied Sciences Wildau, Wildau, Germany
e-mail: daniel.alarcon@th-wildau.de

P. Blaschke
Laboratory for Machine Dynamics and NVH, Technical University of Applied Sciences Wildau, Wildau, Germany
NV Tech Design GmbH, Steinheim, Germany

© Society for Experimental Mechanics, Inc. 2020
M. L. Mains, B. J. Dilworth (eds.), *Topics in Modal Analysis & Testing, Volume 8*, Conference Proceedings of the Society for Experimental Mechanics Series, https://doi.org/10.1007/978-3-030-12684-1_27

263

3. The end of the service life of these vital industrial structures is a region-wide phenomenon that, if not promptly addressed, could affect the entire regional economy.

27.2 Introduction to the Project

Heavy duty overhead cranes are an essential part of the heavy industry complexes described in the previous chapter. These cranes are designed to transport heavy loads along industrial facilities or warehouses. In the experience of the cooperation partner in this project, during decades, these cranes and their rails have been exposed to many different loads, damages and material fatigue processes during operation. Runway beams, those holding the rails where the crane runs on (Fig. 27.1), are especially prone to the generation of cracks due to material fatigue. Replacing these runway beams is an expensive operation: besides the pure replacement costs, the crane simply cannot be operated during the time the runway beams are being replaced. This has in consequence large negative impacts in revenue and plant productivity.

Increased damage incidence in recent years has raised awareness in the Brandenburg heavy industrial sector for a need for continuous condition monitoring [2]. Techniques such as structural health monitoring (SHM) can ensure the long-term load capacity and serviceability of overhead crane runway beams. In addition, the early detection of damages favors planning crane downtimes far in advance, minimizing their economic impact on the plant's economic output.

Common methods of runway rail/beam monitoring include visual inspections, which detect visible local damage. Deformation tests can provide information on the global wear and tear and thus, on the global structural degradation. Implementing SHM techniques has the advantage, for instance, that the damage locations do not have to be known a priori. A SHM system is based on modal system properties, which are acquired in a non-destructive way. The advantages of condition monitoring based on system properties are manifold; e.g., the locations and nature of the damages do not need to be known, or visible. Furthermore, it is not necessary for the measurement sensors to be located near damage points.

A particular case is studied for this paper. In these cases, cracks occur frequently in the upper flange of an I-shaped runway beam during operation. I-shaped beams are an efficient form for carrying bending and shear loads in the plane of the web, but their cross-sections have a reduced capacity in their transverse direction, inefficient in carrying torsion.

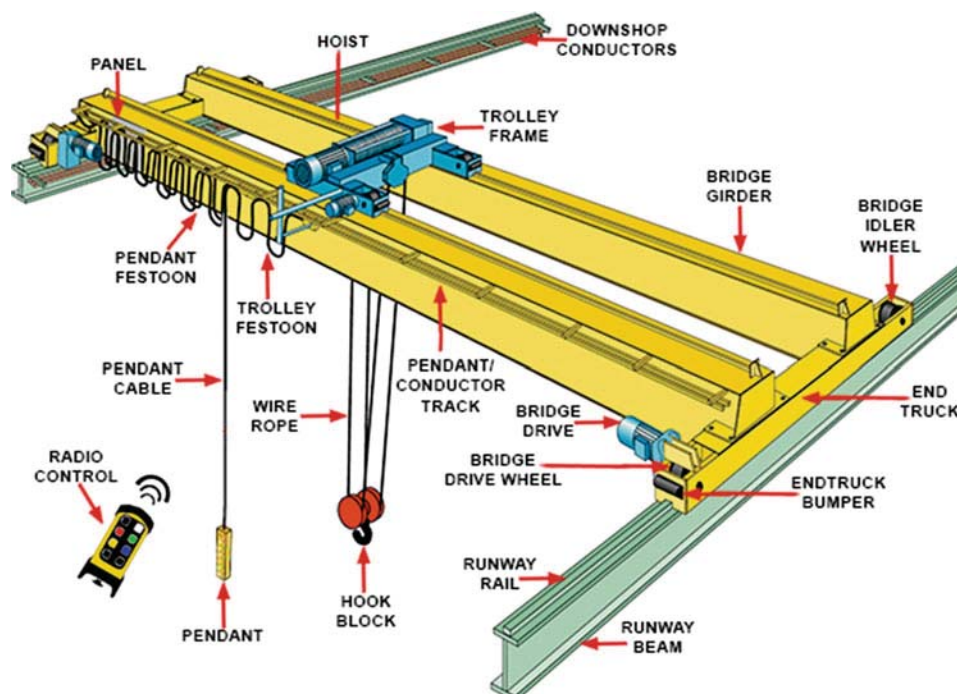


Fig. 27.1 Parts of a bridge crane. This study is centered on runway beams, named at the bottom of the figure (Source: [3])

This paper presents the results of a feasibility study for a vibroacoustic damage detection procedure on bridge crane runway beams. A 2-m beam segment has been dynamically studied and the results used to correlate and validate a Finite Element (FE) model, generated by means of optical scanning. Several damage cases were later simulated in the FE model, evaluating this way the development potential for a vibroacoustic method for damage detection in crane runway beams.

27.3 Materials and Methods

One structure was measured in this project, which is a 2 m long section of a real runway beams supplied by a cooperation partner (Fig. 27.2). In order not to damage the laboratory floor, the runway beam section was supported on wooden blocks and L-profiles as shown at the right side of Fig. 27.2. The influence of the L-profiles was taken in account in the FE model. Both L-profiles contact with the runway beam section at about 300 mm from the runway beam edges. A wooden pallet is visible in the figure below the beam section. It does not contact the beam in the experimental setup and is there mainly for safety purposes.

The dynamic properties of the beam were obtained with two different measurement methods and results were subsequently correlated. One measurement was carried out with a 3D Scanning Laser Doppler Vibrometer mod. PSV-500-3D (Polytec GmbH, Waldbronn, Germany) and the other one with a roving 3-axis accelerometer mod. 356A01 (PCB Piezotronics, Depew, NY, USA).

Given the poor laser reflectivity the railway beam offers, each degree of freedom (DOF) was marked with a small adhesive reflective paper piece. Figure 27.3 shows several measurement setup pictures for clarity. 363 Frequency Response Functions (FRF) were measured, three for each DOF in X, Y and Z direction in both accelerometer and 3D SLDV cases. All DOFs are separated about 200 mm from each other in the Y and Z directions. The 3D SLDV laser heads were positioned at a distance of 3.5 m away from the beam. The roving accelerometer was affixed with paraffin wax on each point. The 3-axis accelerometer was always mounted with the same orientation for data consistency. In both measurements, the beam section was excited by means of the Scalable Automatic Modal hammer SAM2 (NV Tech Design GmbH), applied at the driving point (DOF 55) on the back side of the web with a force of about 300 N. Three averages were needed with an interval of 9 s between impacts to allow the beam vibration to fully decay. For the SLDV tests, data was acquired with the software package PSV 9.3 (Polytec GmbH, Waldbronn), while the accelerometer tests were acquired with a vMeas data acquisition card and software vModal (Maul-Theet GmbH, Berlin). The extraction of modal parameters was carried out with vModal, by manually curve-fitting the obtained FRFs with a generally damped SDOF algorithm.

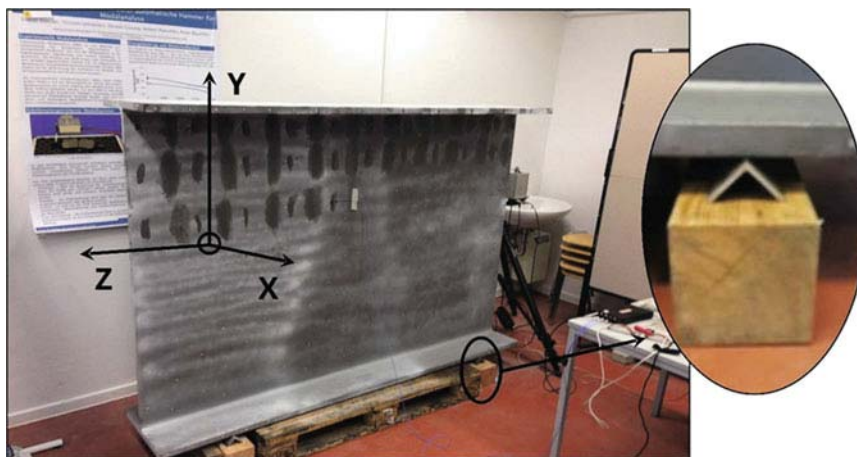


Fig. 27.2 (Left) Accelerometer modal test setup on runway beam section. (Right) Zoomed view of the runway beam section supports

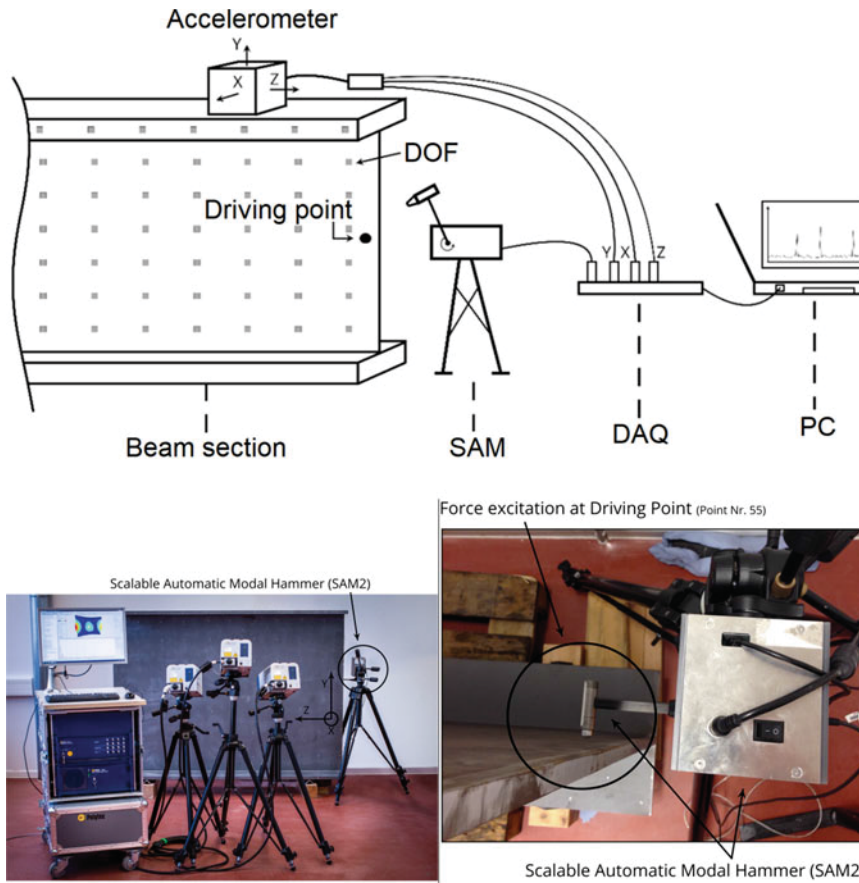


Fig. 27.3 (Top) Experimental setup for the roving accelerometer test. The web and both upper and lower flanges were measured. (Bottom left) Experimental setup for the 3D SLDV test. (Bottom right) Detailed view of the excitation, provided by the Scalable Automatic Modal hammer on the back side of DOF 55

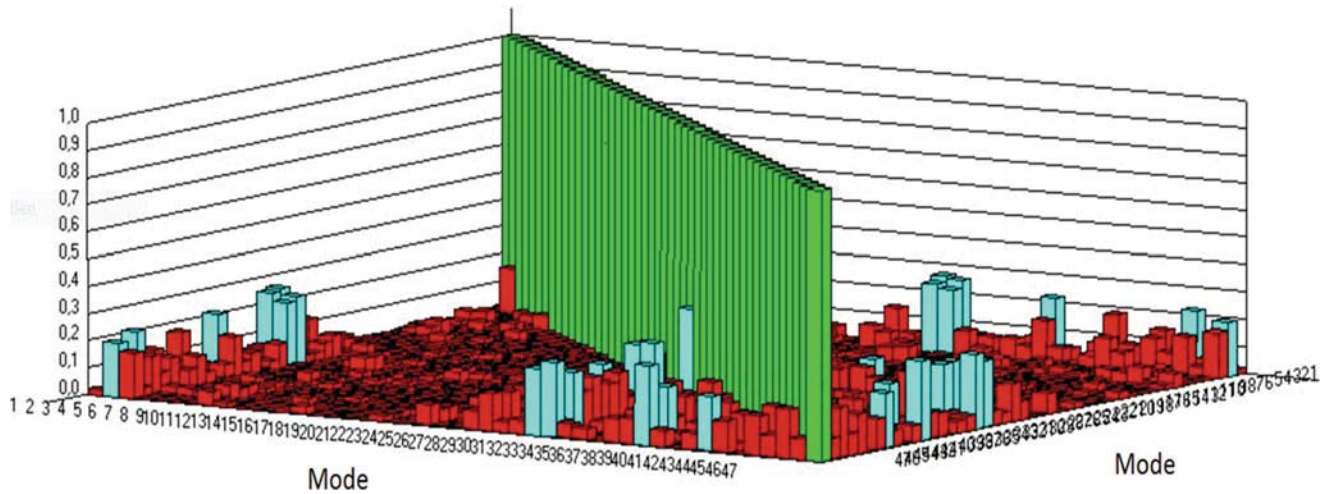


Fig. 27.4 AutoMAC matrix of the measurement using 3D SLDV as output sensor

27.4 Test Results and Discussion

Figure 27.4 shows the AutoMAC matrix for the SLDV test. The AutoMAC for the accelerometer test is similar. It is observed how lower and higher order modes are influenced by spatial aliasing, with very good autocorrelated modes in the middle range.

Table 27.1 Extracted modes from both modal analyses. It is observed how the 3D SLDV procedure offers larger mode sensitivity in lower and higher ranges

Accelerometer		3D SLDV	
Modes	58	Modes	70
Frequency range	11.88–1142.33 Hz	Frequency range	2.99–1578.70 Hz

FRFs obtained by means of 3D SLDV needed re-indexing before they could be correlated with those from the accelerometer measurement, as the data acquisition system assigned different DOF values. A different amount of modes was determined by each study. The evaluation of the two measurement methods covered the following range (Table 27.1).

The comparison of the evaluated data of both measurements extends only over the modes up to 1200 Hz in order to avoid spatial aliasing at higher mode orders, as shown by the AutoMAC. The curve fit procedure is expected to have an influence in the results, as this is a procedure prone to human-influence, especially when highly couple modes are encountered. The lower accelerometer sensitivity to low frequency vibrations, and very prominent 3 Hz rigid body mode, are also clearly observed in the results. The results shown in Fig. 27.5 do not include the first mode in the accelerometer study.

A direct comparison with both modal datasets was carried out as described below, relying on the natural frequency difference (NFD):

$$NFD (EM A_{r,A}, EM A_{i,B}) = \frac{(\omega_{r,A} - \omega_{i,B})}{\min(\omega_{r,A}; \omega_{i,B})} * 100\%$$

Figure 27.6 shows significantly higher deviations of up to 4.3%. For higher order modes, the other eigenfrequencies of the two measurements correlate very well with each other. In total there is an average percentage deviation of $\approx 0.4\%$ across all 46 modes.

The differences between the modes of the two measurement methods could be partly based on slightly different measurement parameters, e.g., the force excitation varied between the two measurements, because the settings were made individually in both cases. Furthermore, there were slight differences at the excitation place.

Figure 27.7 shows the deviations of the respective modes of both measurements in terms of modal damping ratios. The diagram shows that certain mode pairs are very different and present higher deviations. A look at the mode shapes makes it clear why such a deviation and high values occur. For example, the second mode from the accelerometer measurement is very noisy (Fig. 27.5). The 3D SLDV results show some low-quality measurement DOFs in modes 1 and 3 due to bad signal reflectivity, which also contribute to these deviations.

A cross-correlation MAC matrix (XMAC) was generated to compare between both measurements (Fig. 27.8). Several low frequency modes appear poorly correlated due to the reasons stated above. From about 630 Hz the modes of the 3D SLDV measurement are additionally superimposed with a kind of rigid body motion. This vertical motion adds to the concerned mode shape of the beam and dominates these, so the results of the XMAC presents poor correlation at these modes.

27.5 Model Correlation and Fe Model Updating

A Finite Element (FE) was created based on a geometry scan (Fig. 27.9). The aim is to use a validated FE model to simulate different scenarios of damage and to investigate the sensitivity of the runway beam. Generally, the creation of an accurate dynamic FE model is a continuous process and involves various recurring adjustment steps until a certain degree of approximation to reality is achieved. The method requires a fine adjustment of the parameters in each process section. It should be noted that a model is a simplified reflection of reality and it generally does not capture all the attributes of the original, but only those that are relevant.

Due to the continuous optimization in terms of material parameters, boundary conditions and mesh quality, the result is a numerical model with an average natural frequency deviation of about 2.8% for 40 evaluated modes. Figure 27.9 shows the natural frequency difference matrix for the first 10 natural frequencies between the numerical model 3 and the acquired modes of the accelerometer measurements. It can be seen that modes 1 to 3 have the again highest relative deviation.

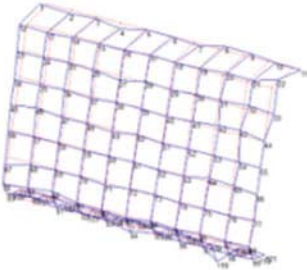
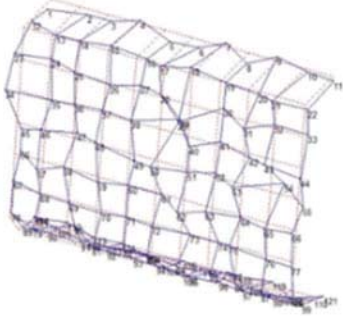
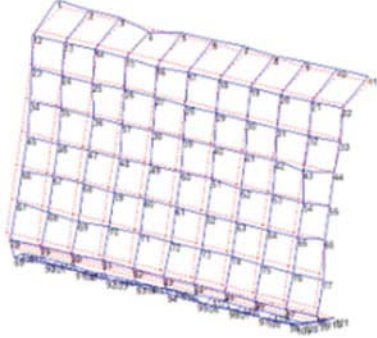
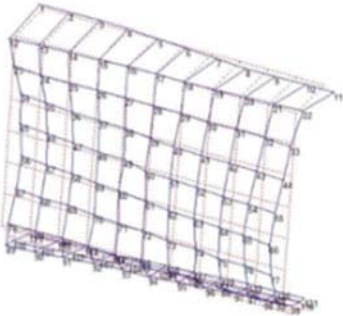
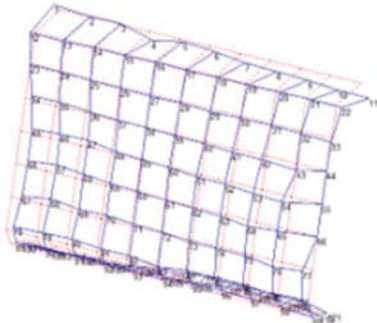
Mode	Piezo	Laser
1. Mode	 $f = 11,88 \text{ Hz} / D = 0,233\% / 1. \text{ Mode}$	 $f = 11,52 \text{ Hz} / D = 0,34\% / 1. \text{ Mode}$
2. Mode	 $f = 26,36 \text{ Hz} / D = 0,10\% / 2. \text{ Mode}$	 $f = 25,24 \text{ Hz} / D = 0,941\% / 3. \text{ Mode}$
3. Mode	 $f = 50,61 \text{ Hz} / D = 0,83\% / 3. \text{ Mode}$	 $f = 48,29 \text{ Hz} / D = 0,775\% / 3. \text{ Mode}$

Fig. 27.5 Direct comparison between eigenfrequencies, damping ratios and mode shapes for both accelerometer and 3D SLDV tests. Note the very noisy mode shape obtained for mode 2 in the accelerometer test. This accelerometer model is rated to work down to 2 Hz, therefore the source of the noise remains unknown

Numerical modal data from ANSYS was exported to FEMTools (DDS, Leuven, Belgium) for a cross-correlation between analytical and experimental data from both accelerometer and 3D SLDV tests. A detailed comparison of the first 10 modes shapes and a classification (clustering) of frequency sectors from all modes were established. Figure 27.10 shows an example of this comparison.

It can be seen that the first three modes of the FEM (Figs. 27.11 and 27.12) show significant deviations in the eigenfrequencies. Besides the reasons stated earlier, spatial resolution has also an impact in this analysis. The assignment of the mode shapes between the EMA and the FE model was visually adjusted because many more modes were extracted by the FE solver. This numerical model with a deviation of less than 5% of the natural frequencies after mode 4, forms a very good basis for the simulation of certain damage situation in the railway beam.

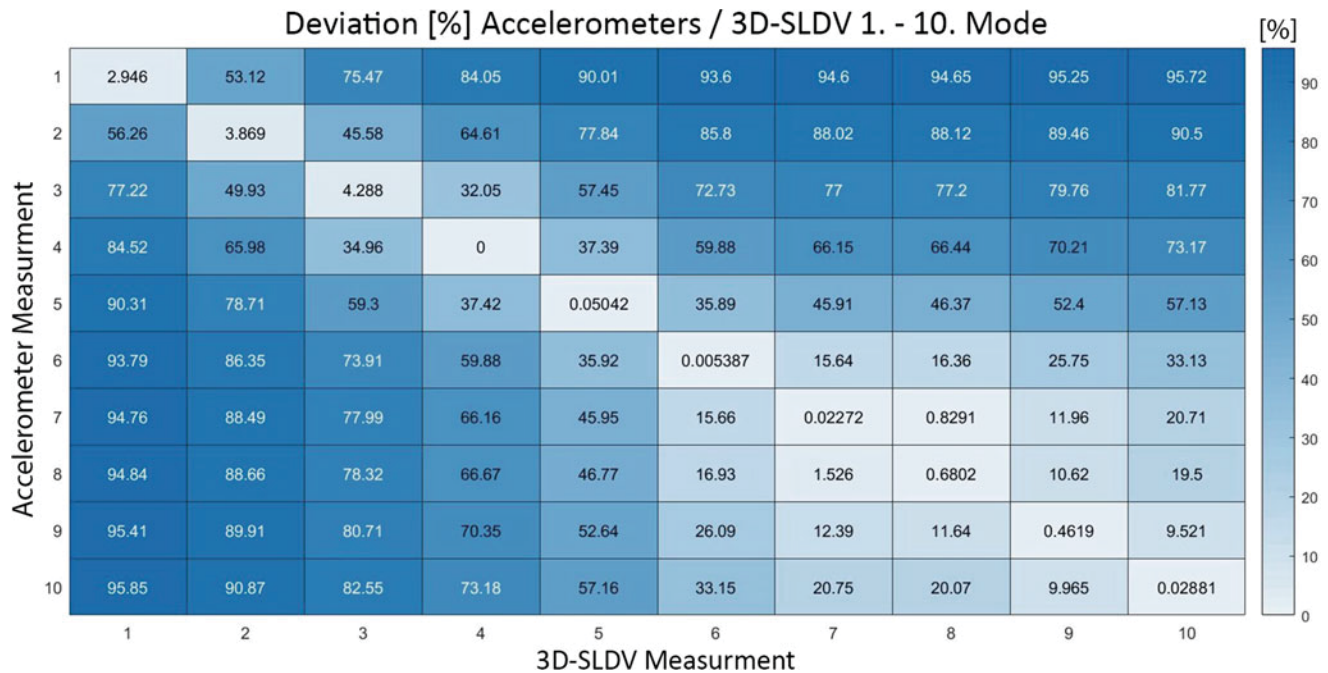


Fig. 27.6 NFD matrix between accelerometer and 3D SLDV tests. Large deviations are observed in modes 1 to 3

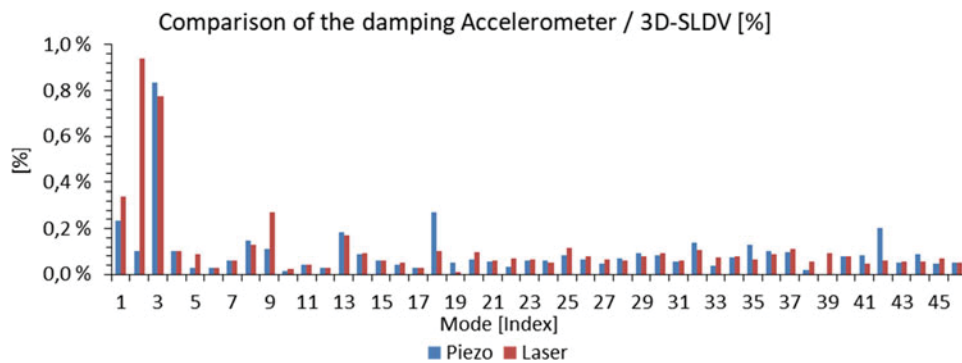


Fig. 27.7 Modal damping ratios comparison between accelerometer and 3D SLDV tests

27.6 Damages Sensitivity Study

According to the experience of the cooperation partner in this project, most of cracks take place in the beam’s upper flanges. One of the aims of this project is to determine whether such damages can be dynamically detected. Due to practical reasons, it is not possible to cause physical damages to the railway beam sections in laboratory scale.

Damages can be described as changes in a healthy system. This can be simulated by applying an external masses and measuring the changes in selected sensitive areas. Numerical and experimental data from this “new” system is to be collected and correlated. Mode shapes are observed and sensitive points are determined in the upper flange. The damages simulation focuses exclusively on the upper flange in this study Fig. 27.13 shows the relationship between DOF sensitivity and mode shape.

To verify the selected sensitive points on the beam, damages were simulated with an added 40 kg mass placed at the top of the upper flange of the beam, on top of DOF 6. Changes in the dynamic parameters are expected (Fig. 27.14).

The investigation of the measuring points follows the cluster of Table 27.2 and the spatial directions X and Y seen in Fig. 27.2. As an example of this analysis, Fig. 27.15 shows the measured FRFs for DOFs 2Y, 4Y and 6Y, with and without mass loading for a Y axis orientation. DOF 6X was set as reference for all FRFs. DOF 2Y presents a higher sensitivity than DOFs 4Y and 6Y.

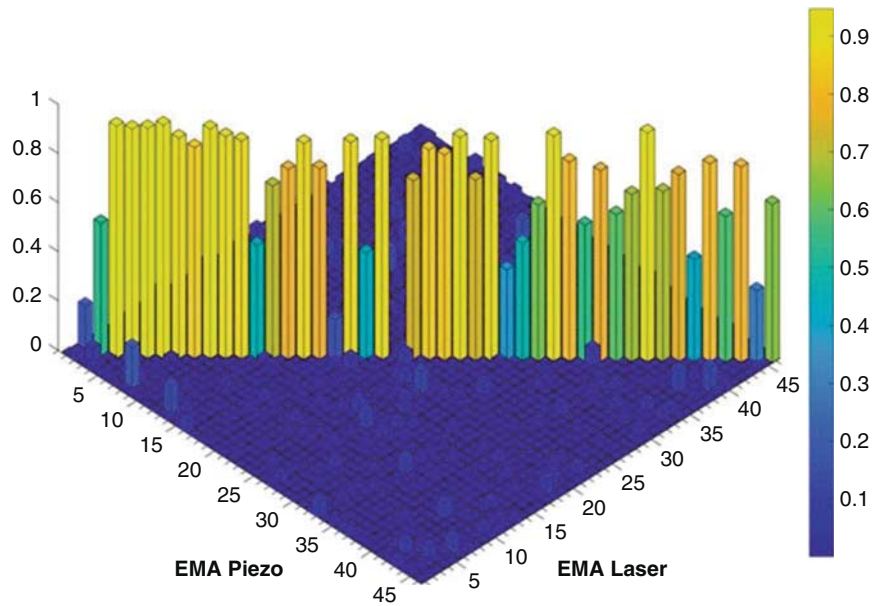


Fig. 27.8 Cross-correlation MAC matrix between accelerometer and 3D SLDV measurements. Low frequency mode pairs 1 and 2 appear poorly correlated

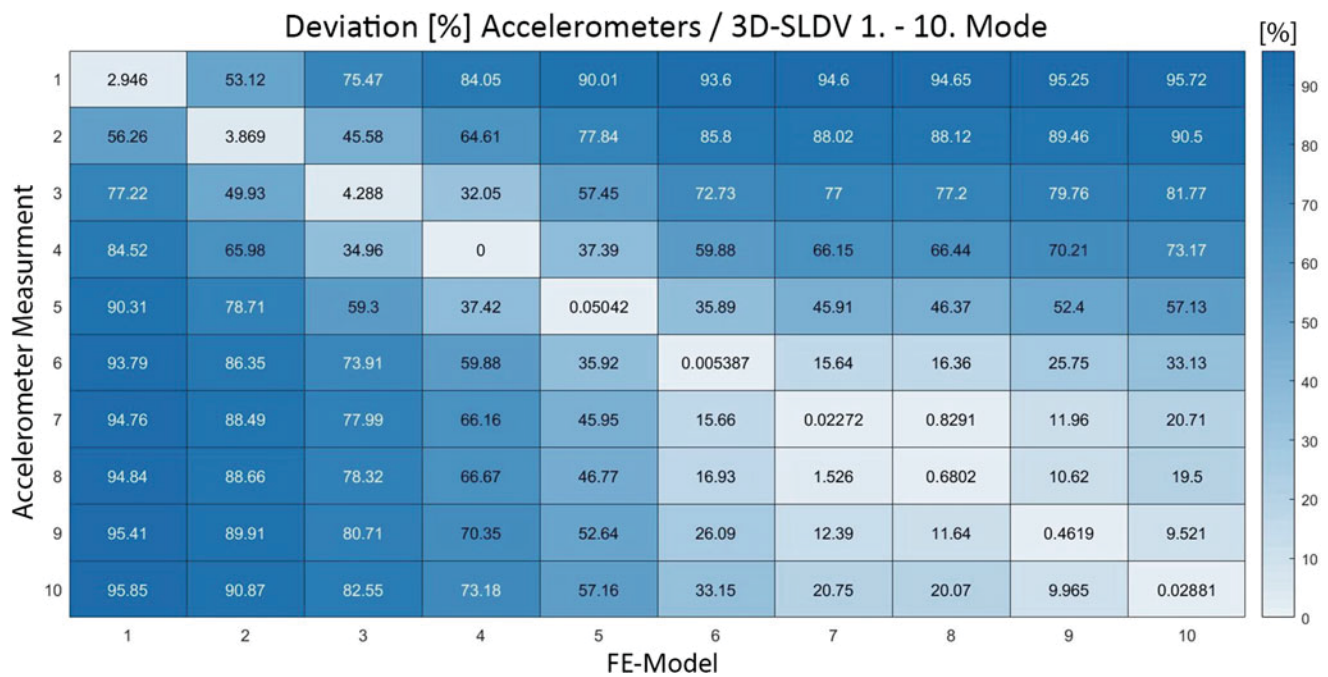


Fig. 27.9 NFD matrix accelerometer and the FE model

In another example, FRFs for DOFs 2X, 4X and 6X present noise all over the spectrum. Mode 5 is increases its amplitude in the loaded case for DOFs 2X and 4X (Fig. 27.16).

The effect of the mass application for the respective displacement, damping or the increase of eigenfrequency amplitudes depends on the associated mode shape and in which region of the upper flange the damage occurs. It is impossible to obtain a uniform statement for all natural frequencies and their peculiarities, because the reaction of each mode is independent of the mode shape.

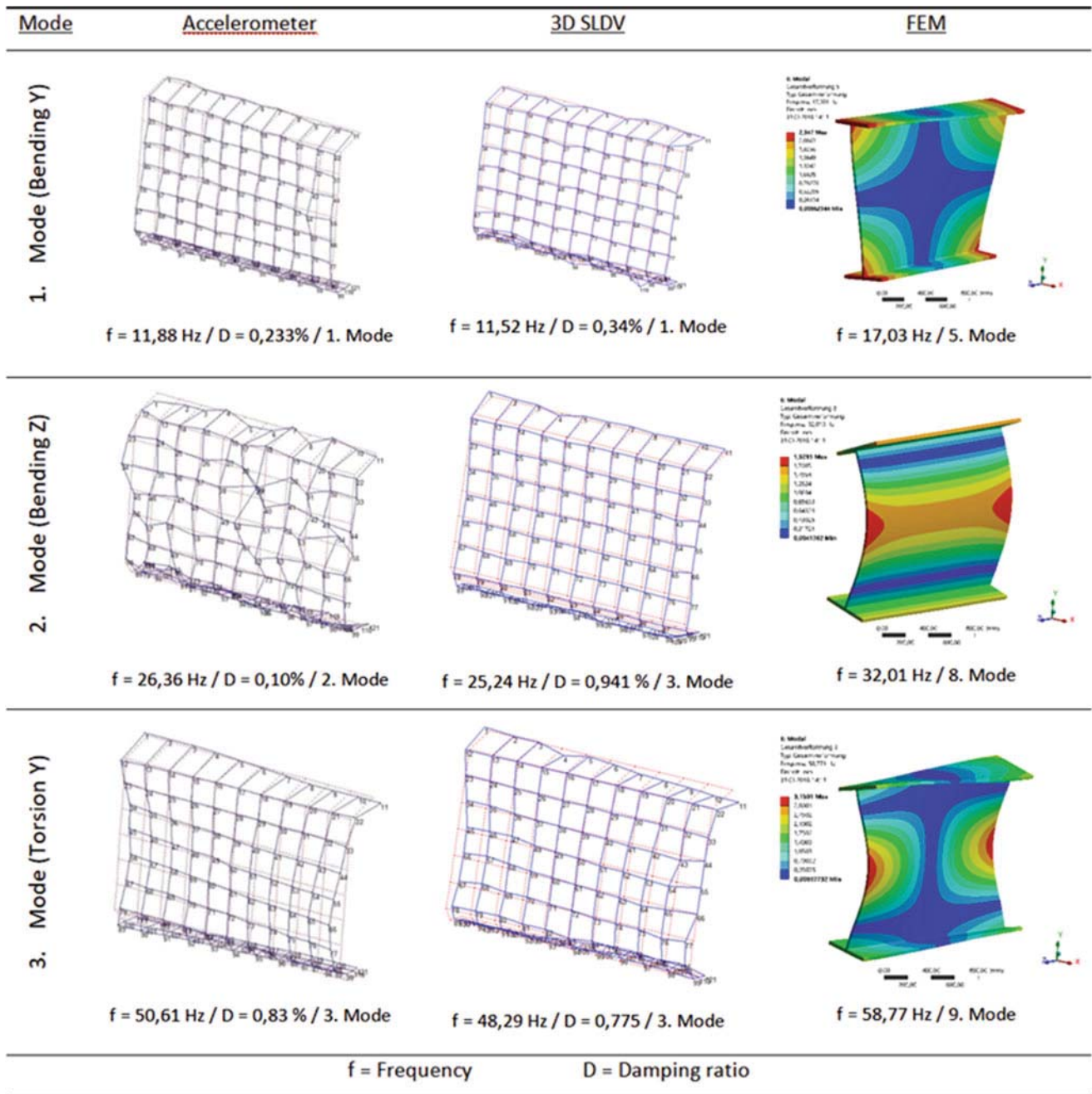


Fig. 27.10 Example of the visual correlation between experimental and numerical mode shapes. Only the three first modes are shown here as an example

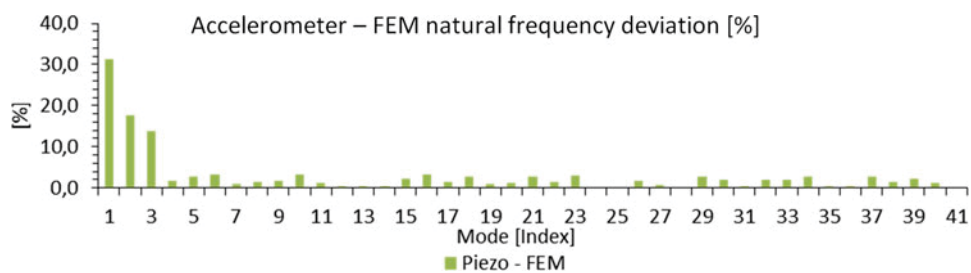


Fig. 27.11 Plot of the relative deviation in eigenfrequencies between accelerometer test and FE model. Note how the highest deviation percentages take place in the first three modes, shown in Table 27.3

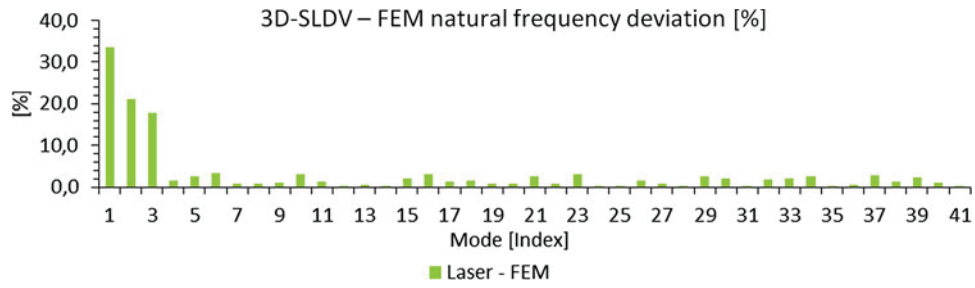


Fig. 27.12 Plot of the relative deviation in eigenfrequencies between 3D SLDV test and FE model. Note how the highest deviation percentages take place in the first three modes, shown in Table 27.3

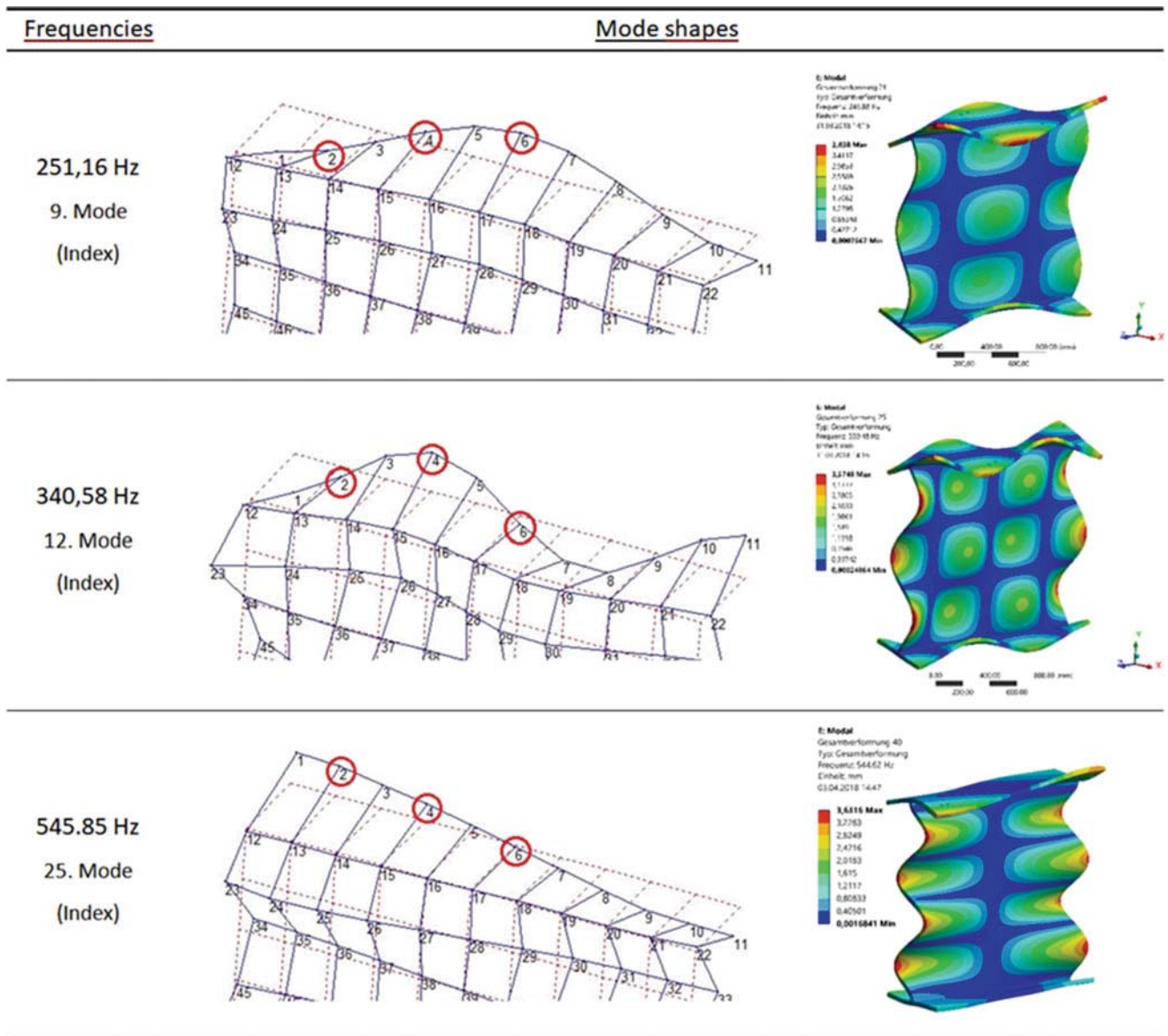


Fig. 27.13 DOF sensitivity for modes 9, 12 and 25. For example, DOF 4Y falls in a node line at mode 9 and thus, is insensitive to this frequency

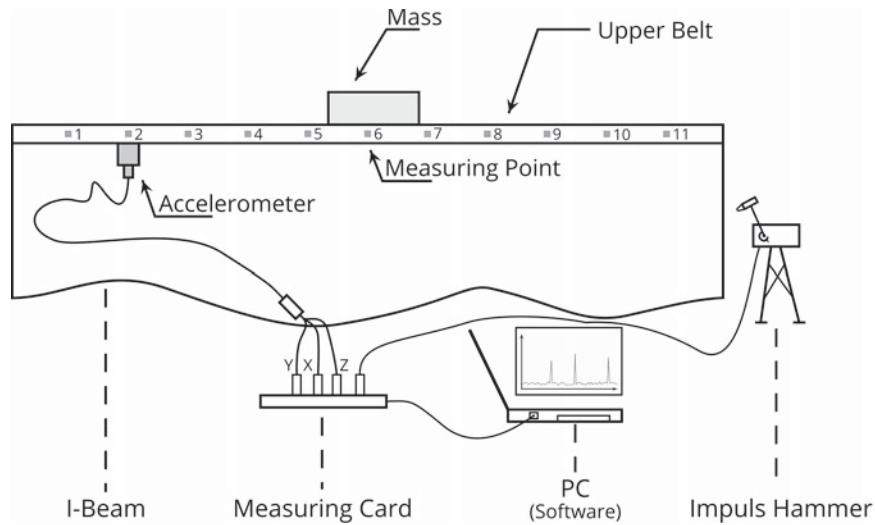


Fig. 27.14 Scheme for the damage detection test setup. Note the addition of the 40 kg mass on top of DOF 6 in this case

Table 27.2 Classification of the modes according to the previously defined frequency ranges (clusters)

Cluster	Bereich	Description
Low frequency modes	10–185 Hz	Vibration area on the web (6 modes)
Medium frequency modes	251–380 Hz	Vibration range on the web and upper flange (6 modes)
High frequency modes	591–733 Hz	Local modes in the web and upper flange (6 modes)

Different damage scenarios can be simulated with a validated FE model of the railway beam section. The aim of the following examination is to determine whether it is possible to detect a crack based by observing eigenfrequency shifts. Four crack dimensional parameters (length, depth, position and width), shown in Table 27.3 and drawn on Fig. 27.17, were correlated with frequency shifts. The obtained eigenfrequencies extracted from the damage simulation were then compared with the natural frequencies of the original FE model. A positive frequency deviation means a reduction in the system stiffness. Several observations can be found in this study.

In the examination of the crack width (ΔW), it can be seen that a width of 5 mm causes the highest frequency deviation (2.04 Hz). The highest natural frequency difference between the three differently simulated crack widths are between the widths of 1 mm and 5 mm and is 0.15 Hz. These results suggest that it is also possible to detect frequency shifts for cracks of less than 1 mm width.

Crack depth (ΔY) seems to be an insensitive parameter in the study if the crack is not fully developed along the flange. A fully developed crack shows significant deviations, of up to 17 Hz, but nevertheless deviations are much lower for a 15 mm crack (2 Hz). No clear shifts are detected for less than 15 mm deep cracks.

The investigations of the crack position (ΔZ) in this railway beam section show this parameter's sensitiveness. Eigenfrequencies are clearly dependent on the position of the crack, and shapes are accordingly influenced. A crack positioned at 230 mm shows only minimal differences because this position is a node line, therefore, there is no significant motion at the cracked area. A crack in the middle of the upper flange at DOF 6 (1050 mm) shows a noticeable shift of the eigenfrequencies at mode 28 (about 360 Hz). The third position at 630 mm (DOF 4) has almost no effect on the lower eigenfrequencies, but higher frequency peaks appear altered. The maximum eigenfrequency deviation at this position is of 20.68 Hz (mode 59). Generally, for all three positions it can be seen that the shifts of the natural frequencies are dependent on the mode shape. At higher frequency ranges, local longitudinal modes appear in the upper Flange, so that it is possible to recognize damages more easily in these ranges.

The longer a crack propagates transversally in the upper flange (ΔX), the larger the shift of natural frequencies is. All simulation variants show how modes 32 (422.89 Hz) and 35 (469.34 Hz) have the highest sensitivity to this parameter (Fig. 27.18). Considering the shapes of both modes 32 and 35, it can be seen that the web vibration dominates with its oscillating shape, but the local motion shape of the upper flange counteracts the elastic deformation. A defect in the upper flange counteracts the web motion and the entire system stiffness is altered. Out of this insight it can be seen why there is an increased sensitivity of the two modes 32 and 35 and the natural frequencies of both shifts.

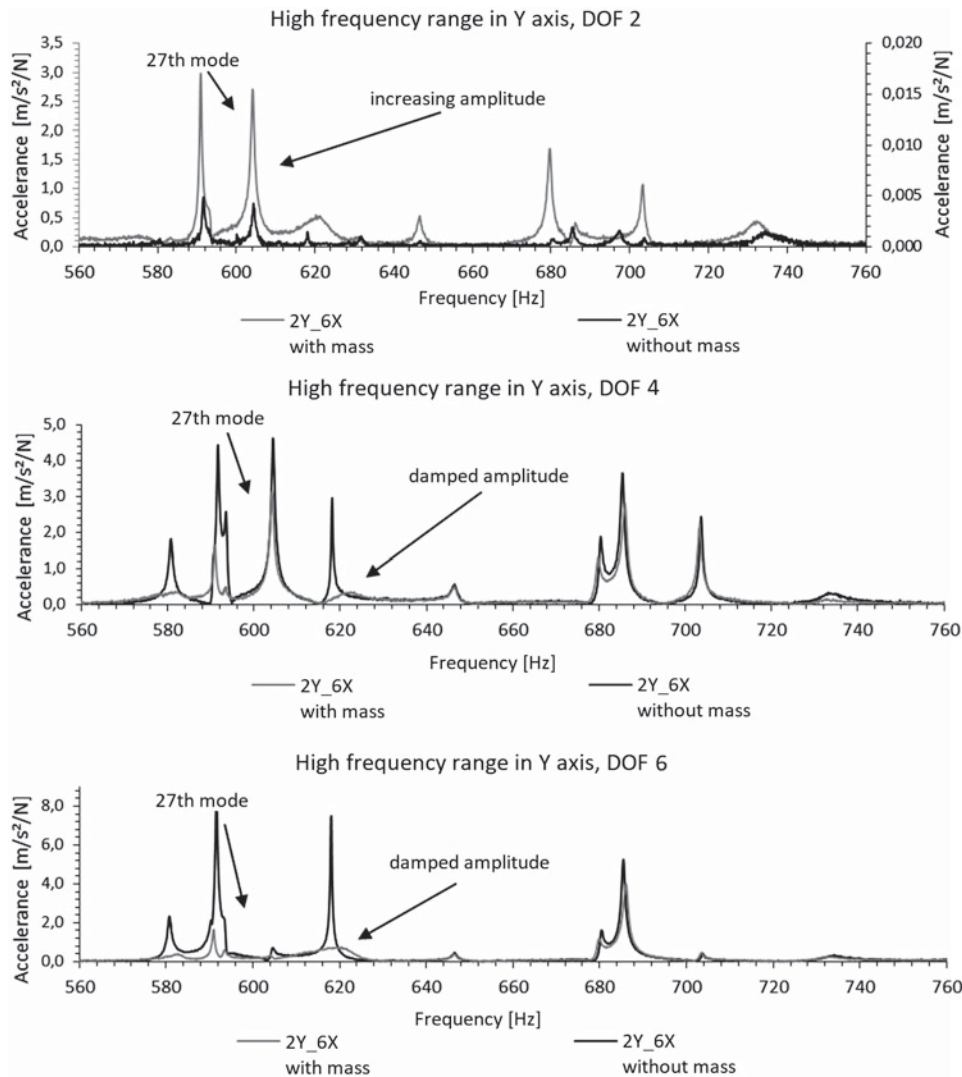


Fig. 27.15 FRFs for loaded and unloaded cases between DOFs 2Y and 6X (top), 4Y and 6X (middle) and 6Y and 6X (bottom), respectively. Large changes are observed in frequency ranges below 660 Hz

27.7 Conclusion

In conclusion, this research project sets the first steps in a larger and longer cooperation project. The present feasibility study includes the vibroacoustic detection of damages to the railway beam section in a laboratory scale and sets the starting point for the ongoing development of a measurement system. The pitfalls of these procedures have been identified in the measurement and cross-correlation phases. A general idea to the damage sensitivities of the studied system has been laid out, and will provide a good insight when dealing with real, 12 m long runway beams.

A working hypothesis is that the mass loading in the middle of the upper flange shows brings significant changes in the system. Figure 27.19 describes how local modes are modified by the mass loading.

Furthermore, some natural frequencies and their damping are shifted and these changes are dependent on the mode shape of the respective mode. Therefore, a sweeping statement is difficult to derive from this investigation because there is a clear dependency between damaged area, frequency shifts and mode shapes.

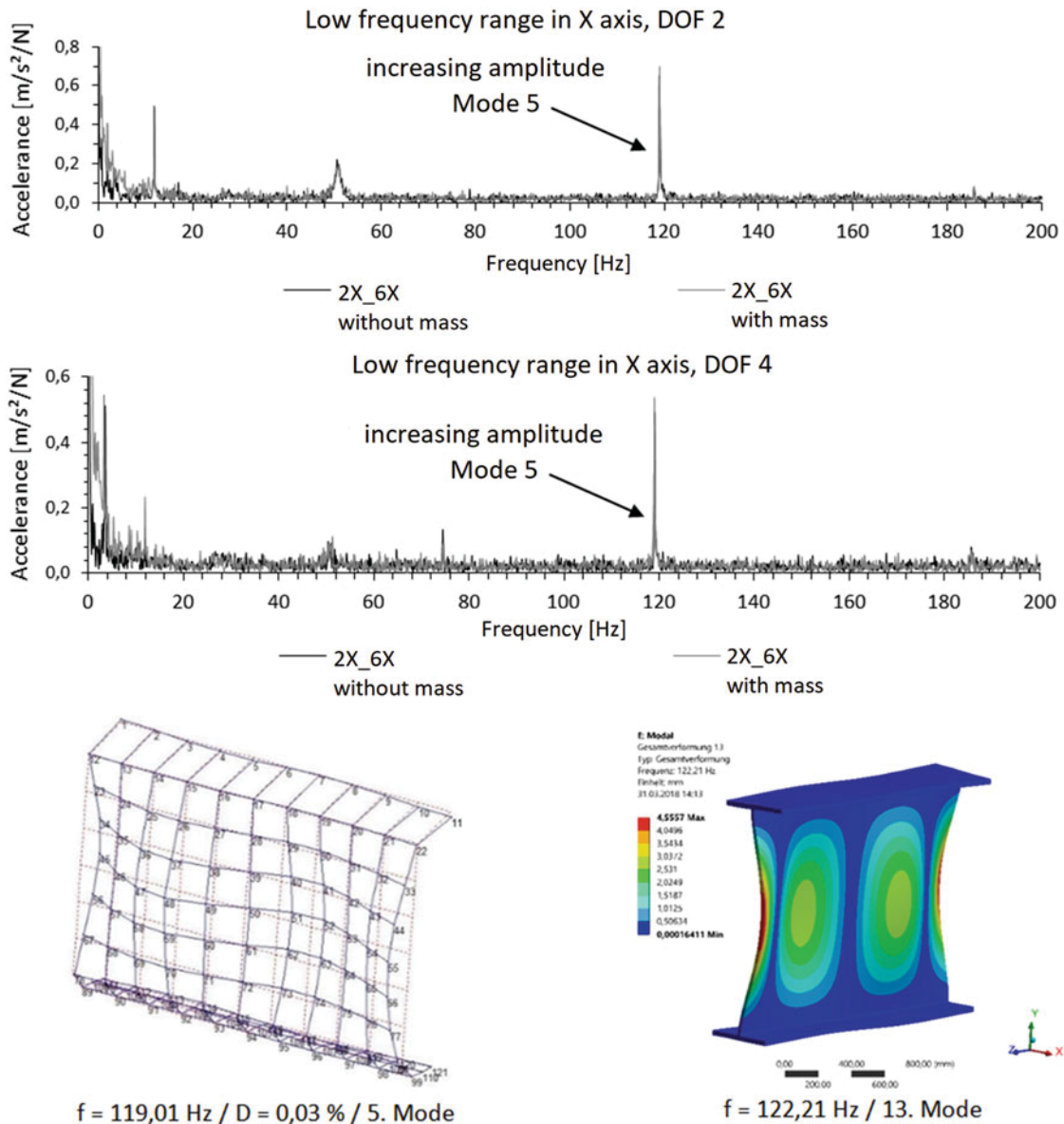


Fig. 27.16 FRFs between DOFs 2X and 6X (top), 4X and 6X (middle) for loaded and unloaded cases. A large increase in amplitude is observed for both cases for mode 5. This mode shape is represented at the bottom of the figure

Table 27.3 Starting parameter values for the damages simulation

Crack length (X)	Crack depth (Y)	Crack position (Z)	Crack width (W)
100 mm	15 mm	1050 mm (measured from the left side)	1 mm

27.8 Further Work

This feasibility study shows that it is possible to detect crack damages on a railway beam laboratory model by studying its dynamic structural behavior. In order to develop a robust structural health monitoring system is it necessary to gain further insight in the following areas:

- Expanding this study to installed railway beams, with the corresponding challenges this implies. These beams are originally 12 m long and techniques such as roving accelerometer can be challenging to apply.
- Extension of the FE model to determine sensitive measurement points
- To document in-situ detection of existing cracks and their location and dimensions

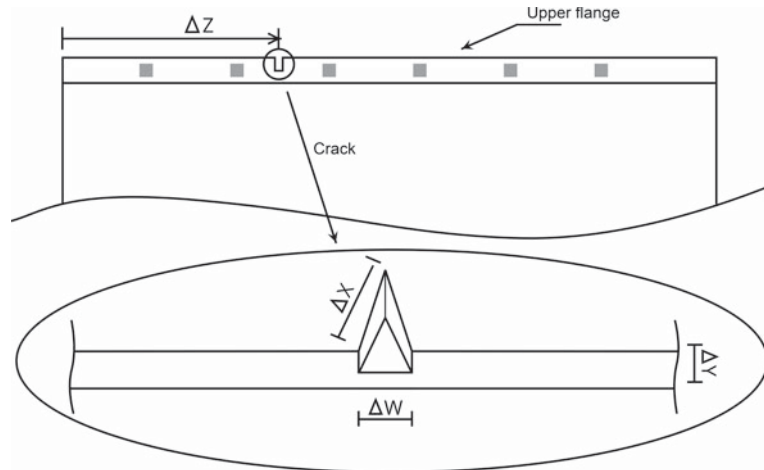


Fig. 27.17 Scheme of the crack parameter variables for the sensitivity study

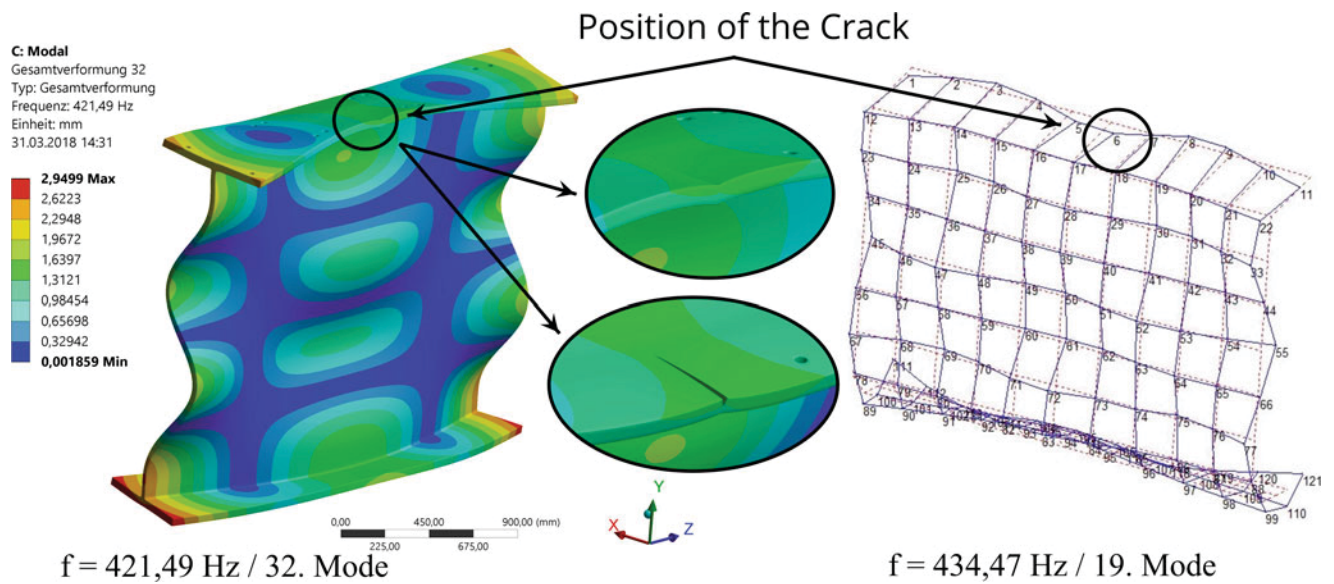


Fig. 27.18 The graphic shows the numerical damaged mode shape (crack at DOF 6) and the unloaded beam for the significant mode 32

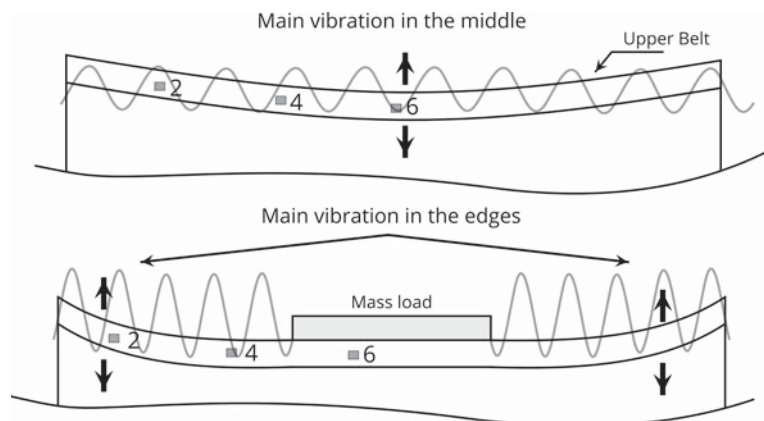


Fig. 27.19 Hypothetical diagram of how local modes in the upper flange are modified by the mass loading

A concept of a crane beam catalog is considered. Each railway beam has its own “identity” in terms of geometry, material parameters and boundary conditions (attachment, support, etc.). Thus, it is not sufficient to verify a beam and to extrapolate the acquired dynamic structural behavior to all other beams. It is necessary to create a feature recognition method on individual parameters and at the same time to compare them with a knowledge database in order to verify the condition of a particular beam.

Acknowledgements The authors would like to express their gratitude to Mr. Torsten Pohlen and Mr. Lars Koczius from ArcelorMittal Eisenhüttenstadt GmbH for their support in the logistics of this project.

References

1. Schlütter, B.: Studieren in Wildau—Ein Hochschul-Porträt in Bildern, MediaService Verlag Bernd Schlütter (2013)
2. Zukunftsagentur Brandenburg: Brandenburgs Schwergewicht—Masterplan für das Cluster Metall Brandenburg, Clustermanagement Cluster Metall Brandenburg (2014)
3. Munck Cranes Inc.: Overhead crane components, online resource. <http://www.munckcranes.com/overheadcranecomponents.asp>. Accessed 20th Oct 2018